Aust. Met. Mag. 47 (1998) 71-81

The tropical circulation in the Australian/Asian region - May to October 1997

S.J. Cleland
Regional Office, Bureau of Meteorology, Darwin, Australia

(Manuscript received December 1997)

A summary of the broadscale tropical circulation from 70°E to 180°, for the six months May to October 1997, is presented. Cool-ENSO conditions prevailed during the previous southern hemisphere summer period. By the start of this summary period there were indicators (e.g., winds and sea-surface temperatures of the near-equatorial Pacific and the southern oscillation index) of a dramatic swing to warm-ENSO conditions. These intensified in the first two months and persisted throughout the period.

The northern hemisphere southwest monsoon system became established over much of Indo-China and the Bay of Bengal during an active phase of the 30 to 60-day intraseasonal oscillation (ISO) in May and advanced over India during June. It had retreated from most mainland areas early in October. Outgoing long wave radiation and low-level wind anomalies indicate a near-average monsoon season over India and Indo-China, but areas around Indonesia and Papua New Guinea were much drier than normal, indicative of the strong warm-ENSO event.

Two coherent active phases of the ISO were evident early in the period, near the middle of May and the end of June. After this time the ISO signal became difficult to interpret, possibly due to the warm-ENSO event suppressing convection in the central longitudes of the region. There may have been up to six cycles of the ISO during the summary period.

A near-average number of tropical cyclones developed during the period. More than 65 per cent of those that affected the northwest Pacific formed east of 145°E, with several also forming in the southwest Pacific, again indicative of the warm-ENSO event.

Introduction

This summary reviews the broadscale tropical circulation in the Australian/Asian region during the period May to October 1997. The area covered is the Darwin Regional Specialised Meteorological Centre (RSMC) analysis domain, that is 70°E to 180°, 40°N to 40°S. The first section uses mostly six-monthly average charts to describe the overall seasonal circulation and anomalies. The second section uses time series to portray variations of the tropical circulation within the season. The final section briefly describes the occurrence of tropical cyclones in the six-month period.

Corresponding author address: Mr S.J. Cleland, Bureau of Meteorology, PO Box 735, Darwin, NT 0801, Australia.

Fig. 1 **SOI time series for ten years to October 1997: monthly values (bars); five-month centred mean values (black line).**

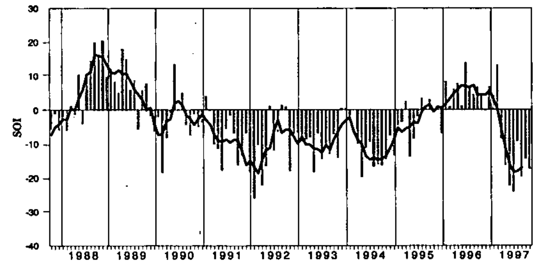

Table 1. Monthly values of Troup's SOI for the period January 1994 to October 1997.

	Jan	*Feb*	*Mar*	*Apr*	*May*	*Jun*	*Jul*	*Aug*	*Sep*	*Oct*	*Nov*	*Dec*
1994	-2	0	-10	-20	-11	-10	-17	-16	-16	-15	-7	-13
1995	-5	-3	+3	-14	-8	-2	+4	+1	+3	-1	+1	-7
1996	+8	+1	+6	+8	+1	+14	+7	+5	+7	+4	0	+7
1997	+4	+13	-8	-16	-22	-24	-9	-20	-14	-17		

Fig. 2 Monthly mean OLR (W m^{-2}), heavy line 240 W m^{-2}, 260 W m^{-2} and above dashed: (a) May 1997; (b) June 1997; (c) July 1997; (d) August 1997; (e) September 1997; (f) October 1997.

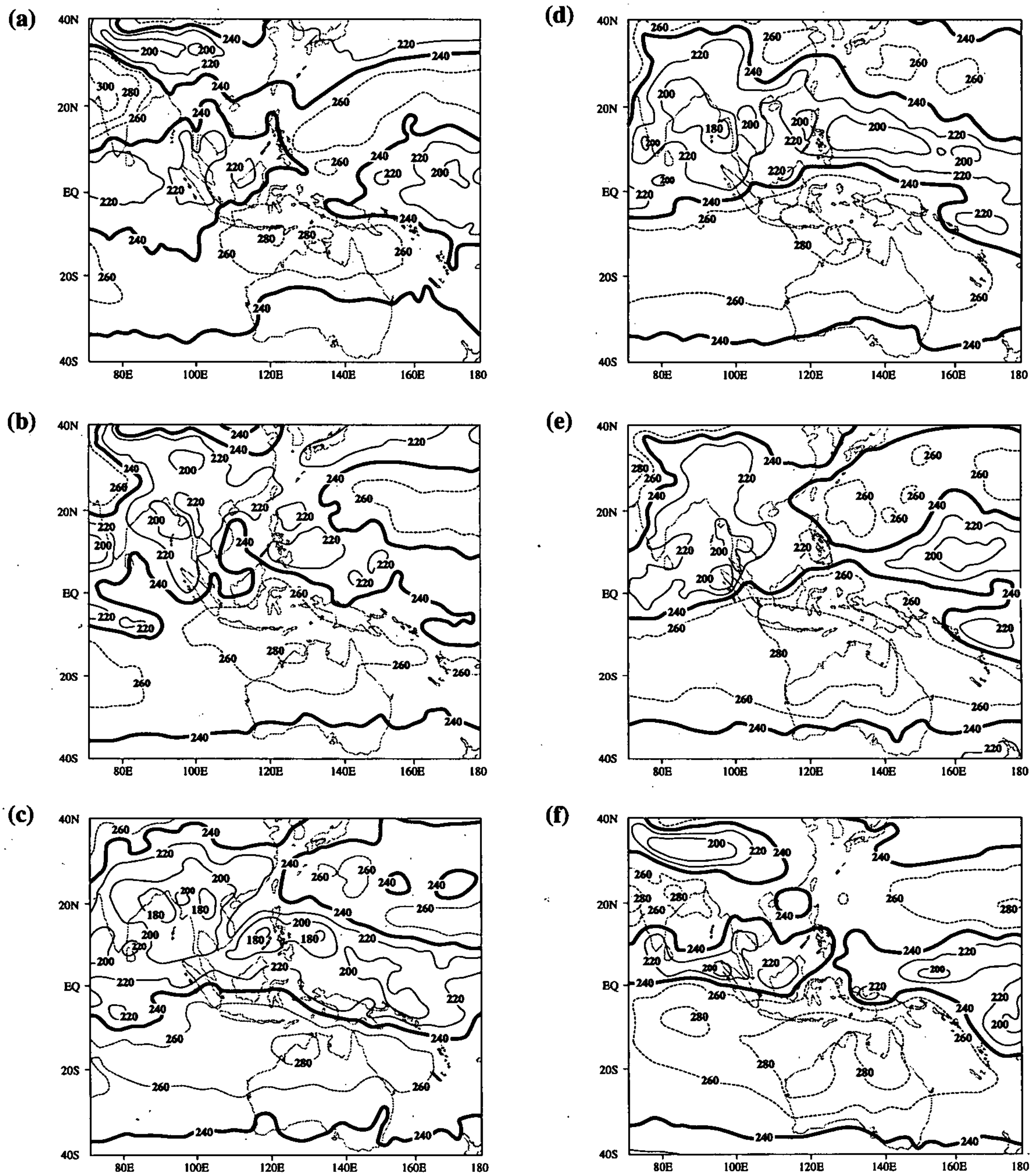

Most of the six-month seasonal charts were constructed using the Darwin RSMC automated operational analysis, TAPS (Tropical Analysis and Prediction Scheme, Puri et al. (1992)). Anomalies are derived from the six-year Tropical Analysis Scheme (TAS) climatology of Lavery et al. (1991). Sea-surface temperature (SST) anomalies were calculated relative to the 1°x1° global SST climatology from the US National Centers for Environmental Prediction (Reynolds and Smith 1995). Further details of the data sources used are listed in the Appendix.

Fig. 3 Monthly OLR anomaly (W m^{-2}), heavy line zero, positive contours dashed: (a) May 1997; (b) June 1997; (c) July 1997; (d) August 1997; (e) September 1997; (f) October 1997. Anomalies from 1979-95 climatology.

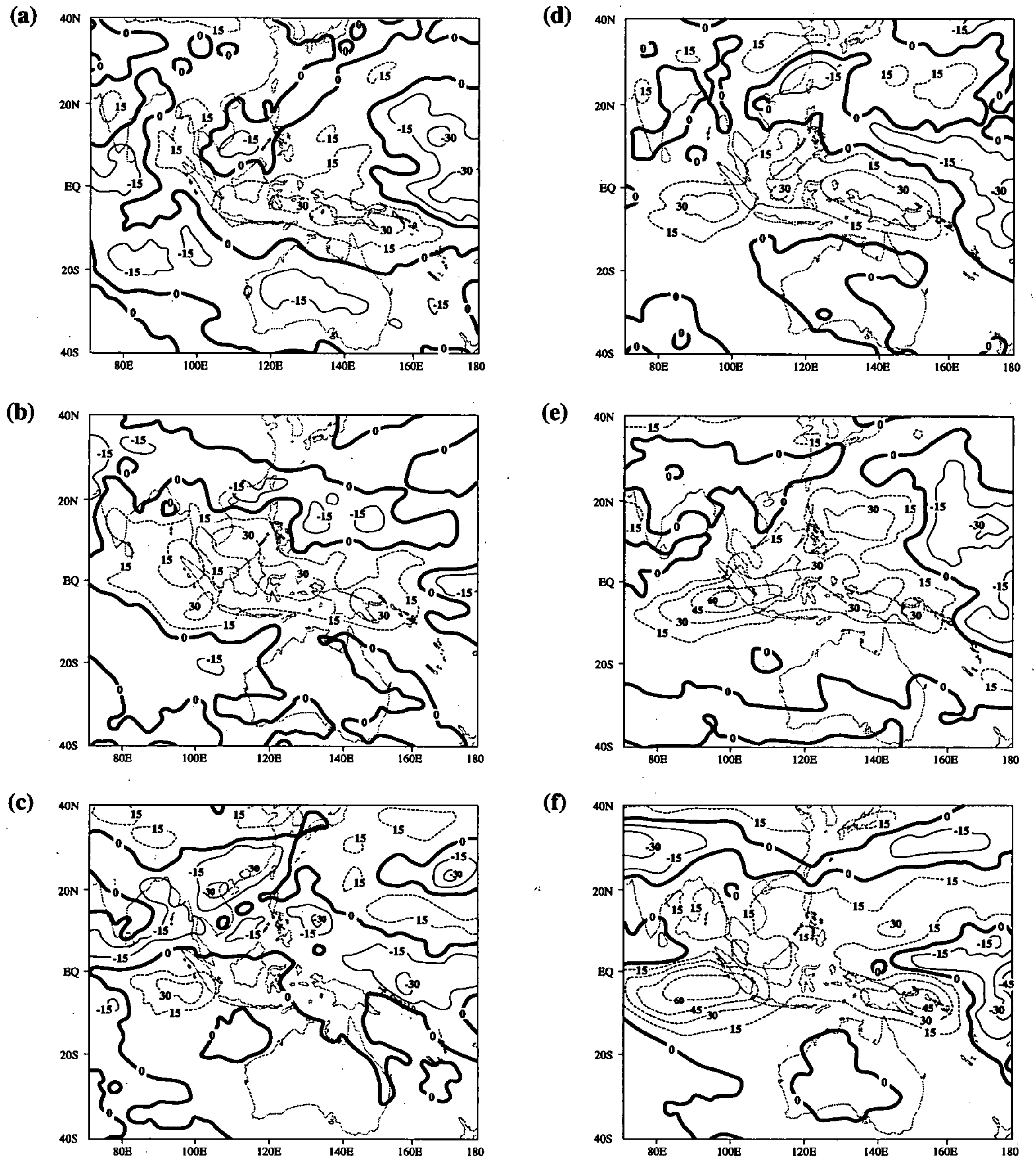

Broadscale seasonal features

After weak cool-ENSO conditions were evident during the previous southern hemisphere summer (Bate 1997) the southern oscillation index (SOI, Table 1, Fig.1) fell rapidly from February, with the June value the lowest recorded for that month since 1905. It remained more than one standard deviation below the long-term mean virtually throughout the period. The five-month running mean was less than -10 from June onwards.

The means and anomalies of outgoing long wave radiation (OLR - used as a proxy for convection) for each month are shown in Figs 2(a) to (f) and 3(a) to (f) respectively. The OLR diagrams depict a very strong warm-ENSO event, with less than average convection over central longitudes of the region over each month of the period except for July, which was mostly near average. The absolute OLR values show that greatest area of convection was displaced from its climatological longitudes near the South China Sea in the months of May, September and October. Absolute OLR values over India and Indo-China were generally near the long-term mean, indicating the monsoon convection in those regions was about average.

Fig. 4 Six-month mean velocity potential (10^6 m^2 s^{-1}), May to October 1997, negative contours dashed: (a) 850 hPa; (b) 200 hPa.

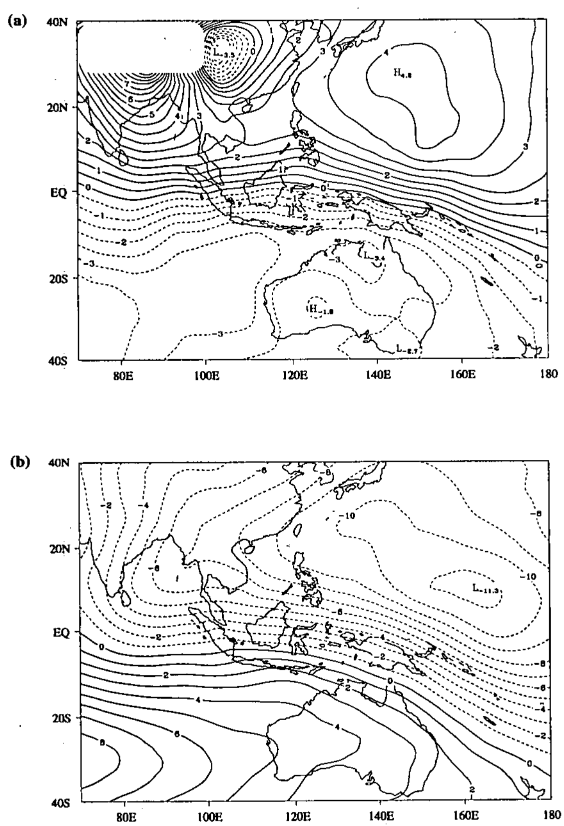

Fig. 5 Six-month SST (°C), May to October 1997: (a) mean, contour interval 1°C; (b) anomaly, contour interval 0.5°C, shaded areas negative.

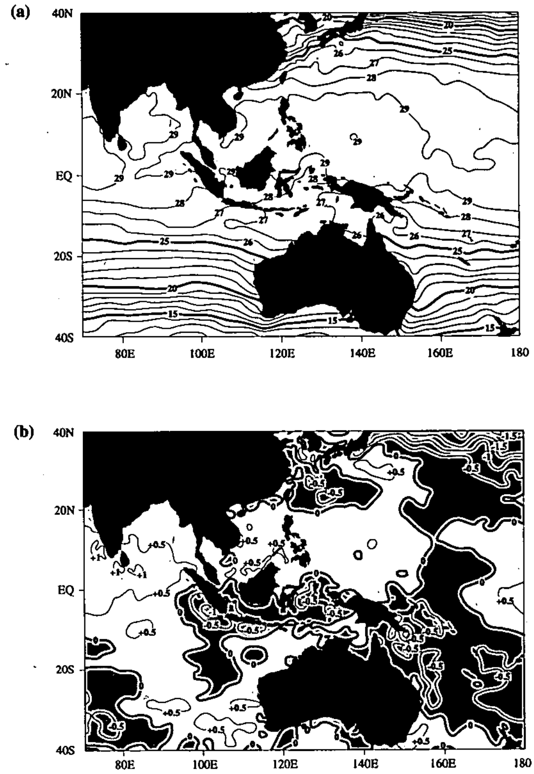

Velocity potential analyses (Fig. 4) show that up-motion, implied by upper-level divergence overlaying low-level convergence, was greatest over the northwest Pacific, where numerous tropical cyclones developed. This eastward shift from the climatological location near the South China Sea is consistent with the strong warm-ENSO event.

Six-month means and anomalies of SSTs are shown in Fig. 5. The strongest anomalies of the region were observed in the mid-latitude northwest Pacific. In tropical areas the vast majority were within 1°C of the long-term mean. Small exceptions were areas greater than +1°C anomaly near India and less than -1°C off the west coast of Sumatra. It is thought that the latter was largely due to upwelling from stronger than average easterly winds; however, it is likely that forest-fire smoke during the later part of the summary period

Fig. 6 Six-month MSL pressure (hPa), May to October 1997: (a) mean, contour interval 2 hPa; (b) anomaly, contour interval 1 hPa, shaded areas and dashed contours negative.

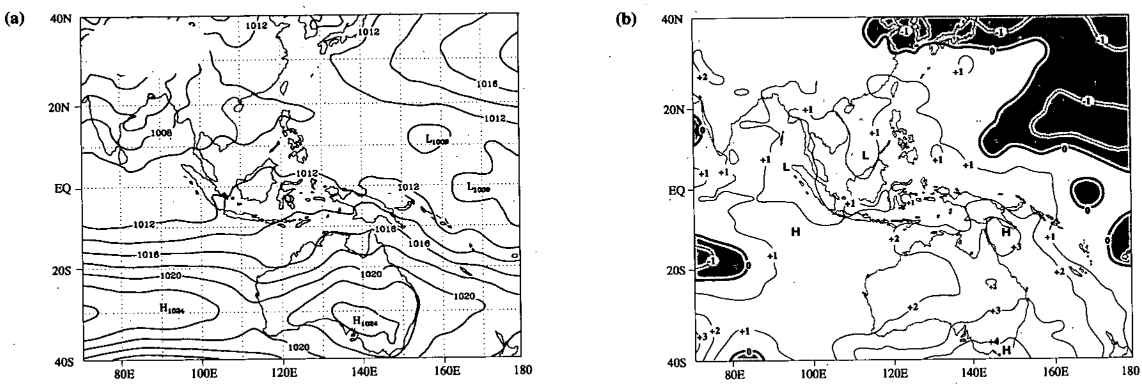

Fig. 7 Six-month 850 hPa wind field, May to October 1997: (a) mean, isotach (dashed) interval 5 m s^{-1}; (b) anomaly, areas greater than 5 m s^{-1} shaded.

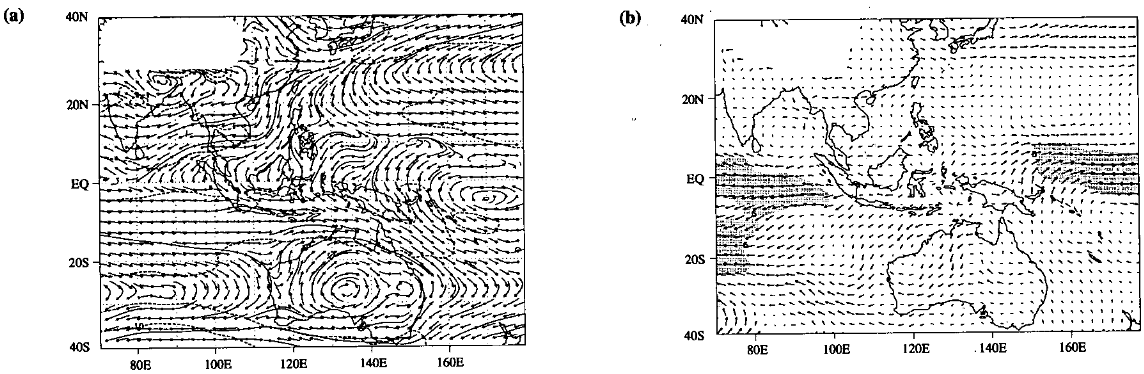

Fig. 8 Six-month 200 hPa wind field, May to October 1997: (a) mean, isotach (dashed) interval 10 m s^{-1}; (b) anomaly, areas greater than 10 m s^{-1} shaded.

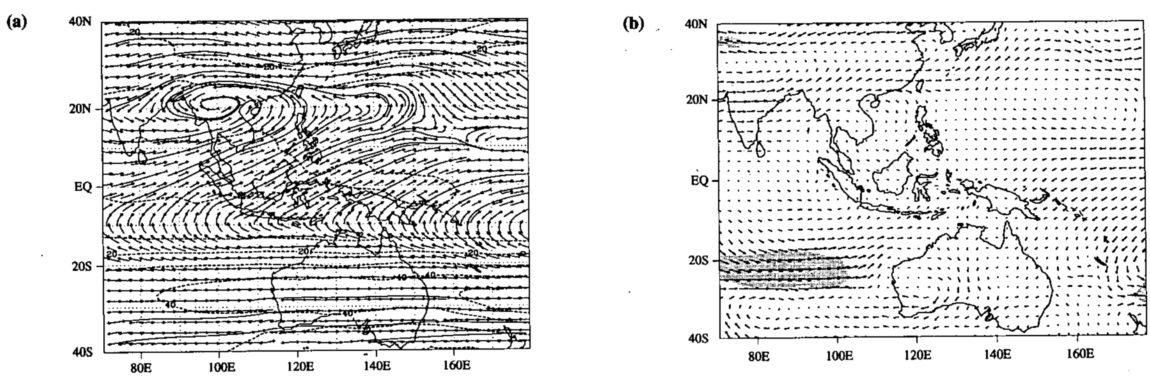

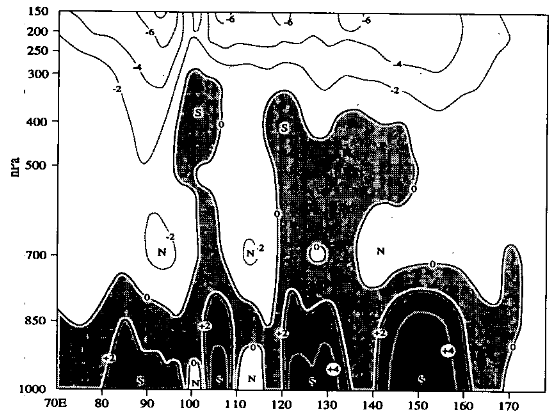

Fig. 9 **Equatorial cross-section of six-month mean meridional wind, May to October 1997; contour interval 2 m s^{-1}, positive (southerly) shaded, negative contours dashed.**

interfered with satellite reception and resulted in cooler than actual temperatures being recorded. There were considerably larger SST anomalies east of the RSMC area, where the eastern Pacific near-equatorial cold tongue was virtually non-existent for the majority of 1997. Hence, warm anomalies exceeding 5°C were observed in parts; this being one of the major indicators of the 1997 warm-ENSO event. The cool anomalies about the southwest Pacific and through parts of Indonesian waters, albeit relatively small, are also consistent with warm-ENSO conditions,

Mean sea-level pressure (MSLP) is shown in Fig. 6. The vast majority of the RSMC area recorded pressures greater than climatology, including New Zealand, Australia, Southeast Asia and India. Negative anomalies were seen in mid-latitude areas east of Korea, and also in the tropical northwest Pacific, east of 140°E. This latter area incorporated the genesis of numerous powerful typhoons, particularly in the latter months of the period.

Streamline/isotach analyses and vector anomalies at 850 hPa are shown at Fig.7. The climatological pattern for the six-month period (not shown) has an easterly

Fig. 10 **Time-longitude sections, latitude band 5°S-15°S, 1 May1997 (day 121) to 31 October 1997 (day 304), of five-day running mean: (a) 200 hPa velocity potential (10^5 m^2 s^{-1}); (b) OLR (W m^{-2}), black circles denote time and longitude of TC genesis events, crosses denote TC genesis events poleward of the latitude band; (c) MSLP anomaly (hPa).**

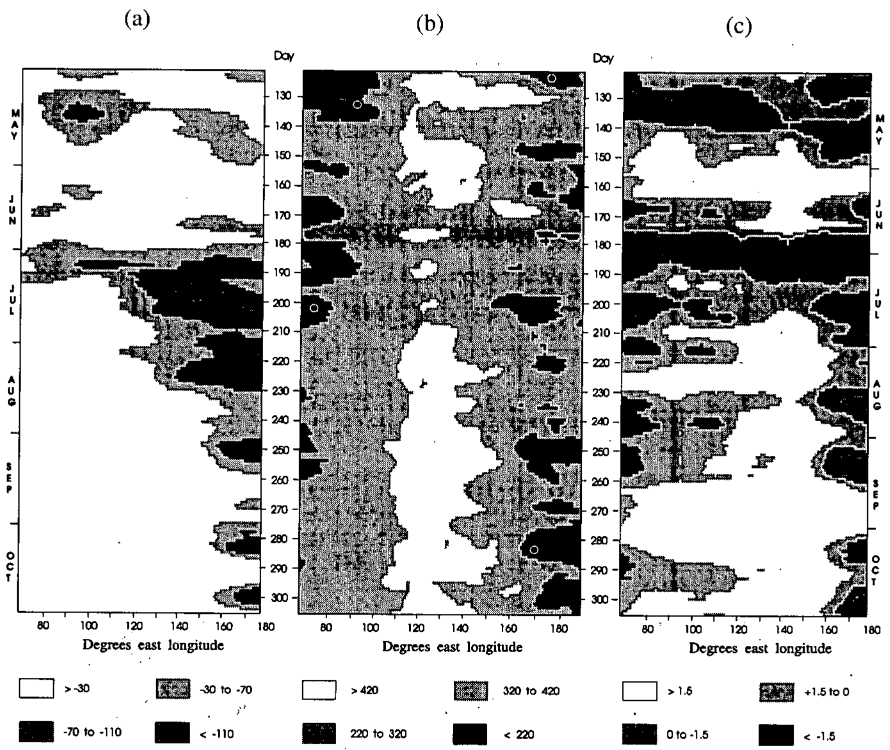

Fig. 11 **Time-longitude sections, latitude band 5°S-5°N, 1 May 1997 (day 121) to 31 October 1997 (day 304) of five-day running mean: (a) 200 hPa velocity potential (10^5 m^2 s^{-1}); (b) OLR (W m^{-2}); (c) MSLP anomaly (hPa).**

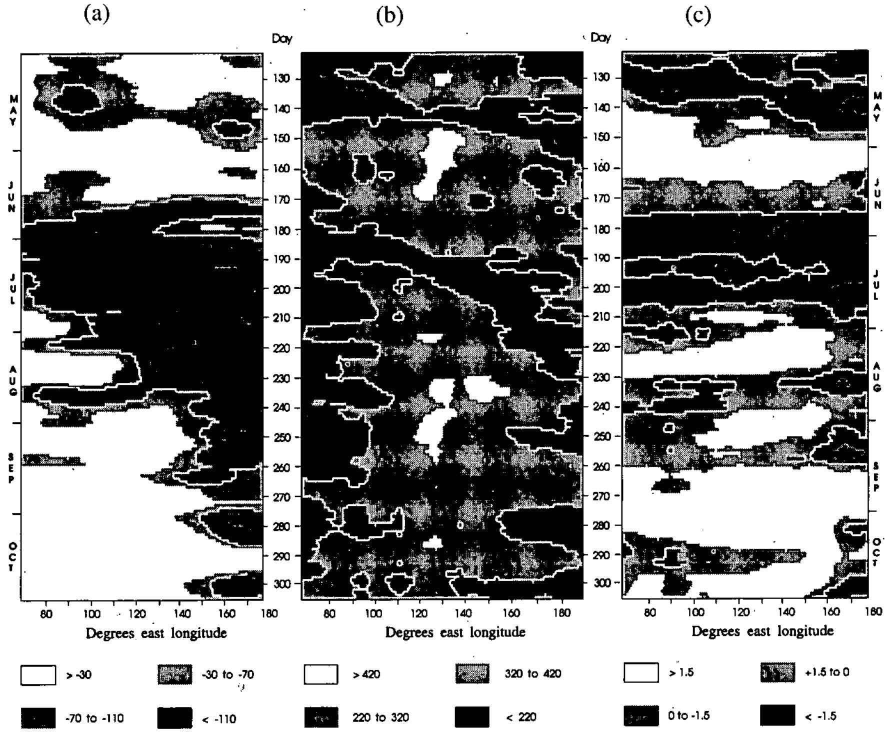

Fig. 12 **As for Fig. 10, except latitude band 5°N-15°N.**

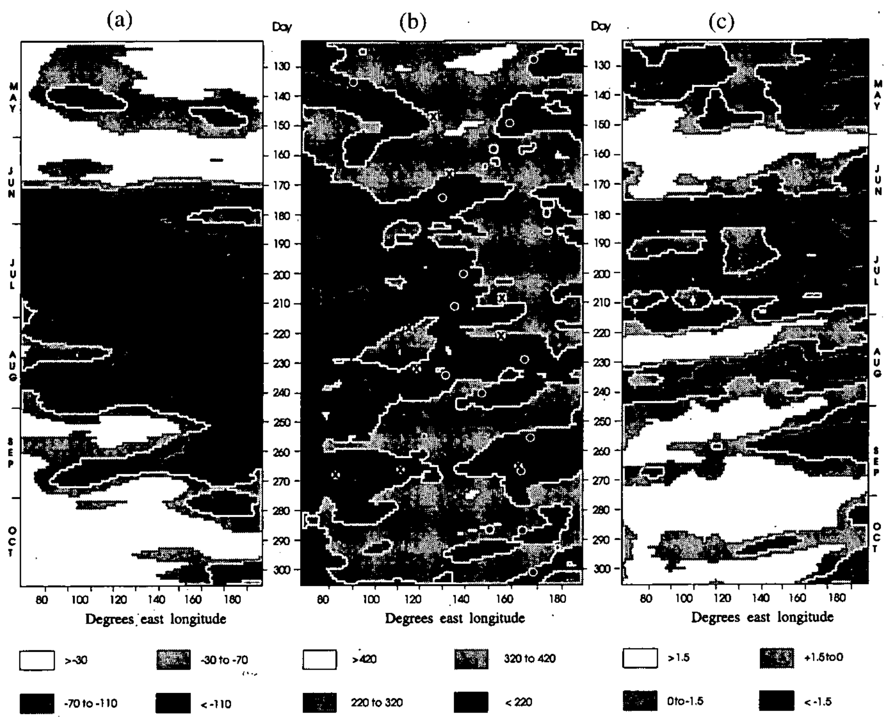

Fig. 13 MSLP for two tropical stations in each hemisphere, normalised then passed through a 40-day Butterworth filter, 50 per cent response at 23 and 70 days: (a) southern hemisphere, thin line Cocos Island, thick line Darwin; (b) northern hemisphere, thin line Singapore, thick line Yap.

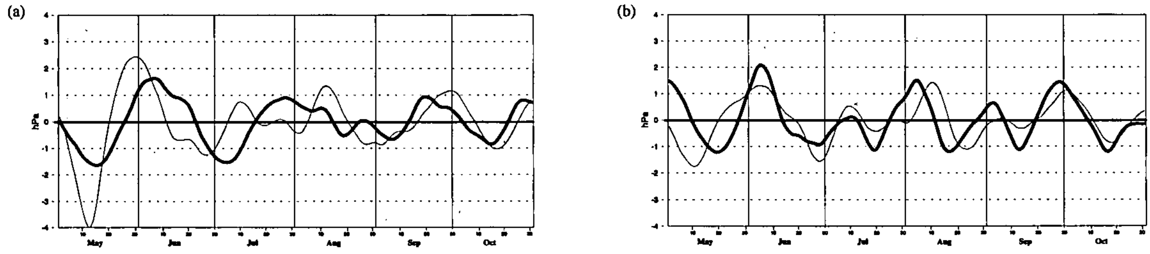

Fig. 14 Tropical cyclone tracks, May to October 1997. Solid line denotes system reached severe tropical cyclone/typhoon intensity; dashed line denotes system reached only tropical cyclone/storm intensity.

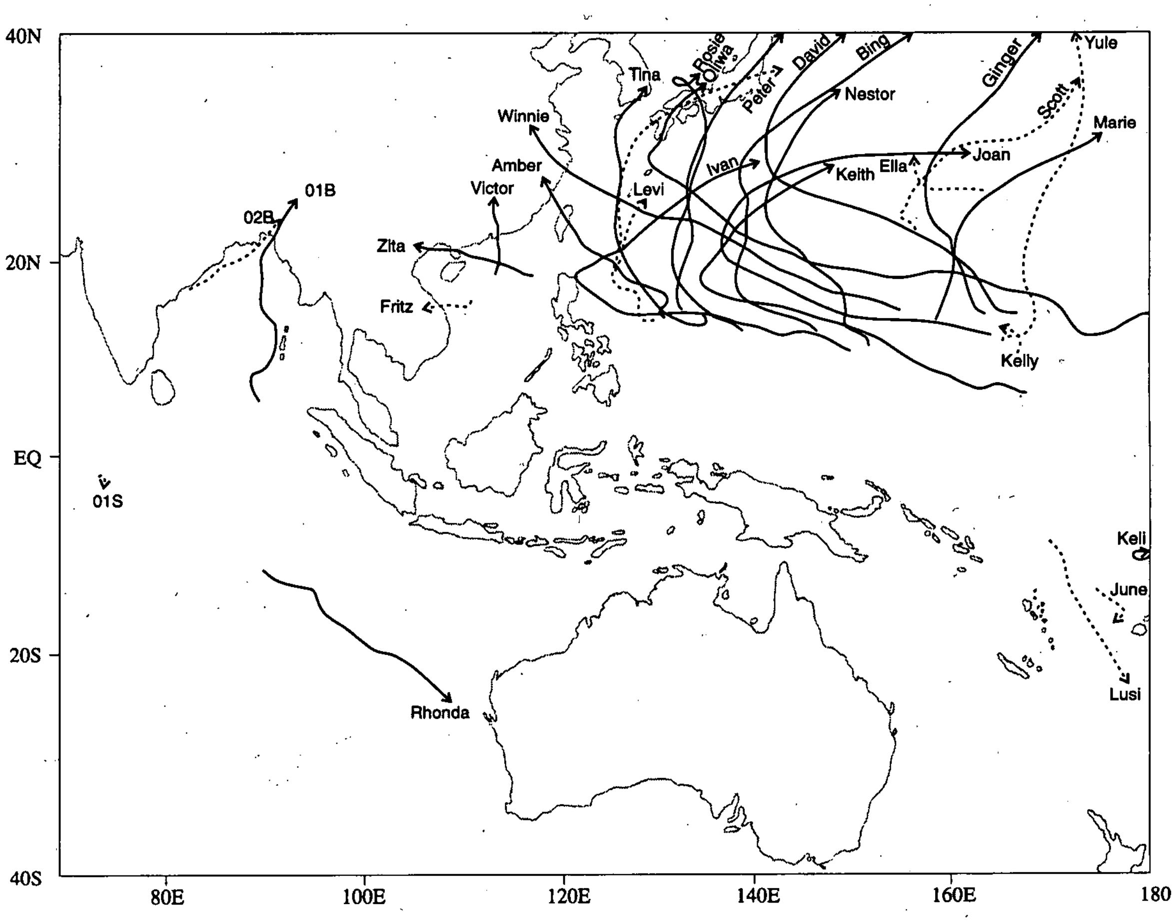

Table 2. Tropical cyclones within the Darwin RSMC area, May - October 1997. TC = tropical cyclone, TS = tropical storm, STC = severe tropical cyclone, Ty = typhoon, * = pressure given by warning agency.

Name	*Dates (UTC) at TC intensity in Darwin RSMC area*	*Maximum 10-min. mean wind (while in Darwin RSMC area) $m\ s^{-1}$ (knots)*	*Estimated minimum MSLP (hPa)*	*Warning agency*
NW Pacific / South China Sea				
Kelly (TS)	08 May-09 May	20 (39)	991	Guam
Levi (TS)	27 May-29 May	18 (35)	994	Guam
Marie (Ty)	29 May-02 Jun	40 (78)	954	Guam
Nestor (Ty)	07 Jun-14 Jun	63 (122)	898	Guam
Opal (Ty)	15 Jun-20 Jun	46 (90)	945*	Manila
Peter (TS)	23 Jun-28 Jun	31 (60)	975*	Tokyo
Rosie (Ty)	19 Jul-27 Jul	60 (117)	905*	Manila
Scott (TS)	27 Jul-02 Aug	20 (39)	991	Guam
Tina (Ty)	30 Jul-09 Aug	41 (80)	950*	Tokyo
Victor (Ty)	01 Aug-03 Aug	33 (65)	968*	Hong Kong
Winnie (Ty)	09 Aug-19 Aug	63 (122)	898	Guam
Yule (TS)	17 Aug-23 Aug	25 (48)	984	Guam
Zita (Ty)	20 Aug-23 Aug	33 (65)	970*	Hong Kong
Amber (Ty)	22 Aug-29 Aug	46 (90)	945*	Hong Kong
Bing (Ty)	28 Aug-04 Sep	56 (109)	915	Guam
Oliwa (Ty)	04 Sep-16 Sep	63 (122)	898	Guam
Cass[1]				
David (Ty)	12 Sep-19 Sep	43 (83)	950	Guam
Ella (TS)	22 Sep-23 Sep	18 (35)	994	Guam
Fritz (TS)	23 Sep-25 Sep	26 (50)	985*	Hong Kong
Ginger (Ty)	24 Sep-30 Sep	65 (126)	895	Guam
Hank[1]				
Ivan (Ty)	13 Oct-25 Oct	51 (100)	930*	Manila
Joan (Ty)	14 Oct-24 Oct	72 (139)	872	Guam
Keith (Ty)	28 Oct-08 Nov	72 (139)	872	Guam
Bay of Bengal/North Indian Ocean				
01B (STC)	15 May-20 May	51(100)	940	Guam
02B (TC)	25 Sep-27 Sep	31 (61)	974	Guam
South Indian Ocean (70°E-105°E)				
Rhonda (STC)	12 May-16 May	46 (90)	940*	Perth
01S (TC)	21 Jul-21 Jul	20 (39)	990	Guam
South Pacific Ocean (165°E-180°)				
June (TC)	03 May-05 May	26 (50)	985*	Nadi
Keli (STC)	11 Jun-12 Jun	36 (70)	963*	Nadi
Lusi (TC)	09 Oct-12 Oct	26 (50)	985*	Nadi

Notes.
1. *Cass* and *Hank* were not considered by Darwin RSMC to have reached TC intensity.

flow throughout the tropical Pacific east of 140°E, and a southern hemisphere near-equatorial trough further west. However, the chart for this summary period has twin near-equatorial troughs over the Pacific, with westerly anomalies exceeding 7 m s^{-1} in the near-equatorial region in between. Further west, southeasterly winds prevailed over southern hemisphere tropical waters, with the near-equatorial turning in the northern hemisphere. Consequently easterly anomalies were evident in the near-equatorial Indian Ocean, of a similar magnitude to the westerly anomalies seen in the Pacific. The resulting pattern was one of low-level wind anomalies diverging from the central RSMC area, indicating a relative weakening of up-motion in the Walker circulation of this region, typical of a warm-ENSO event. Near-equatorial anomalies east of the RSMC area (not shown) are consistent with this, showing westerly anomalies and, in parts, a complete reversal of the climatological easterlies for much of the summary period.

Streamline/isotach analyses and vector anomalies at 200 hPa are shown at Fig. 8. These show subtropical westerlies in each hemisphere stronger than normal. The divergent upper flow in the western Pacific near the date-line was more pronounced than the long-term mean, shown by diverging anomalies over the region. The long-term mean also shows a closed circulation in the southern hemisphere subtropical ridge of this region, but this cell was displaced east of the date-line during this warm-ENSO summary period.

The diagram depicting the cross-equatorial component of the flow (Fig. 9) shows there were two small areas where the southerly component was deeper than the long-term mean (not shown); these being regions over Sumatra and north of Papua New Guinea (PNG) where the six-month mean southerly component was up to the 300 hPa level. The low-level southerly component was stronger than the long-term mean in the low levels from the western border of PNG to Bougainville, over the Moluccas, and the area between Borneo and Sumatra, consistent with the enhanced monsoon trough in the northwest Pacific east of 140°E. The upper northerlies over the western Pacific were stronger than normal, with greater upper-level divergence consistent with the warm-ENSO conditions. Elsewhere the upper-level cross-equatorial component was mostly close to climatology.

Intraseasonal variability

Figures 10 to 12 show time/longitude plots of (a) 200 hPa velocity potential, (b) OLR and (c) MSLP anomaly, averaged over 10° latitude bands, across the Darwin RSMC longitude range. Figure 13 shows filtered MSLP for selected tropical stations. An active phase of the 30 to 60-day intraseasonal oscillation (ISO) around the middle of May, and again near the end of June, was apparent in all of the time-longitude plots and filtered MSLP series. After this time the ISO signal was less pronounced and difficult to interpret, but near-equatorial and northern hemisphere time/longitude plots, supported by the filtered MSLP series for Singapore and Yap, indicate weak active phases of convection occurred near the middle of each month July to October. The southwest monsoon became established over much of Indo-China and the Bay of Bengal during the active phase of the ISO in the middle of May. Over most of India onset occurred during June. The monsoon had retreated from most mainland areas early in October.

The southern and northern OLR plots (Figs 10(b), 12(b)) also indicate the date and longitude of tropical cyclone genesis events in their respective hemispheres. There was some clustering of TC genesis events about active phases of the ISO; however there were also several events outside of the widespread periods of convection.

Tropical cyclones

Tropical cyclones (TC) are defined as having maximum ten-minute mean winds greater than 17 m s^{-1}, or named systems. Operational tracks are shown in Fig. 14, while Table 2 lists TCs in order of occurrence within the various basins, showing duration and estimated maximum intensity details. Tracks are from the near real-time publication *Darwin Tropical Diagnostic Statement* (DTDS, see Appendix) and are based on Darwin RSMC operational manual analyses, with limited post-analysis in a few cases. Maximum wind details were obtained from the operational warnings issued by the agencies responsible. Following WMO guidelines (Neumann 1993), winds are assumed to be averaged over ten minutes, except those from Joint Typhoon Warning Center, Guam (JTWC), which uses one-minute means. Darwin RSMC uses a conversion factor of 0.88 to relate one-minute to ten-minute means, and this was applied to warnings issued from Guam. Since most agencies use the unit of knots in warnings, wind speeds are shown in Table 2 in knots as well as m s^{-1}. Where not given by the responsible warning agency, minimum pressures were estimated for operational analyses using the relationship of Atkinson and Holliday (1977). Details may be derived from JTWC warnings when warnings were not received from the responsible local warning agency. A brief discussion and further details of each of the cyclones can be found in DTDS for the relevant month.

During May to October 1997, 30 tropical cyclones were analysed within the Darwin RSMC analysis domain. This was close to the long-term mean in most regions, though there were more than normal in the southwest Pacific. Twenty-three developed in the northwest Pacific, compared to the mean of 22.7. Fifteen of these (65 per cent) formed east of 145°E. Two formed in the north Indian Ocean where the long-term mean is 2.8. The long-term mean for the south Indian Ocean plus the south Pacific is 2.2, but six formed during this period; two in the south Indian Ocean and an unseasonable four in the South Pacific (one of these being east of the Darwin RSMC area of responsibility). All of the southwest Pacific systems formed east of 160°E, consistent with the warm-ENSO conditions which prevailed during the summary period.

Acknowledgments

The author would like to express sincere thanks to Rob Porteous for his drafting of figures and to Gordon Jackson for the six-month average charts from both TAPS and the SST analysis scheme. Thanks are also expressed to the Climate Prediction Center, Washington DC, for permission to use OLR figures.

Appendix

Data sources used in this summary were:

Darwin Tropical Diagnostic Statement, May to October 1997 (issued monthly), and *Weekly Tropical Climate Note*, 6 May to 4 November 1997. Bureau of Meteorology, GPO Box 735, Darwin, NT 0801, Australia.

MSLP and upper wind data from Darwin RSMC real-time Tropical Analysis and Prediction Scheme (TAPS, Puri et al., 1992). Anomalies derived from a six-year climatology of the Tropical Analysis Scheme (TAS, Lavery et al. 1991).

OLR figures from *Climate Diagnostics Bulletin*, May to October 1997, issued monthly by Climate Prediction Center, W/NP52, 4700 Silver Hill Rd, Rm 605, Stop 9910, Washington, DC, 20233-9910 USA.

Sea-surface temperature analysis derived from Melbourne Specialised Oceanographic Centre operational global analysis. Includes blended in situ and satellite data, 1°C resolution. The 1°x1° global SST climatology from the US National Centers for Environment Prediction (Reynolds and Smith 1995) was used to calculate anomalies.

Tropical cyclone climatology for the northwest Pacific, south Indian and South Pacific Oceans calculated from figures given in Etro and Bassi (1996). For the north Indian Ocean the climatology is from Mandal (1991).

Velocity potential data from the Australian Bureau of Meteorology's GASP model (Global Assimilation and Prediction System, Bourke et al., 1990).

References

Atkinson, G.D. and Holliday, C.R. 1977. Tropical cyclone minimum sea level pressure/maximum sustained wind relationship for the western north Pacific. *Mon. Weath. Rev., 105*, 421-7.

Bate, P.W. 1997. The tropical circulation in the Australian/Asian region - November 1996 to April 1997. *Aust. Met. Mag., 46*, 237-46.

Bourke, W., Seaman, R., Embery, G., McAvaney, B., Naughton, M., Hart, T. and Rikus, L. 1990. The BMRC global assimilation and prediction system. *ECMWF Seminar Series: Ten years of medium-range weather forecasting*. 4-8 September 1989, 221-52.

Etro, J.F. and Bassi, J.P. 1996. *1995 Annual Tropical Cyclone Report*. Joint Typhoon Warning Center, Guam. US Naval Pacific Meteorology and Oceanography Center West, Joint Typhoon Warning Center, PSC 489, Box 12, FPO AP 96536-0051, USA, 289 pp.

Lavery, B.M., Davidson, N.E., Karoly, D.J. and McAvaney, B.J. 1991. A climatology of the western Pacific region based on the Australian tropical analysis scheme. *BMRC Research Report No. 28*, Bur. Met., Australia, 26 pp.

Mandal, G.S. 1991. Tropical cyclones and their forecasting and warning systems in the Indian Ocean. *Technical Document WMO/TD - No. 430* (Report No. TCP-28), WMO, Geneva, 430pp.

Neumann, C.J. 1993. The global tropical cyclone forecasting network. In: Global Guide to Tropical Cyclone Forecasting. *Technical Document WMO/TD - No. 560* (Report No. TCP-31), WMO, Geneva.

Puri, K., Davidson, N.E., Leslie, L.M. and Logan, L.W. 1992. The BMRC tropical limited area model. *Aust. Met. Mag., 40*, 81-104.

Reynolds, R.W. and Smith, T.M. 1995. A high resolution global sea surface temperature climatology. *Jnl climate, 8*, 1571-83.